New experimental and numerical methods to characterise the attenuation of a shock wave by a liquid foam

M. MONLOUBOU[a], J. LE CLANCHE[a], S. KERAMPRAN[a]

a. ENSTA Bretagne, UMR CNRS 6027, IRDL, F-29200 Brest, France ;
martin.monloubou@ensta-bretagne.fr

Résumé

Les mousses liquides, dispersion d'une phase gazeuse au sein d'une phase liquide, sont utilisées dans de nombreux domaines de la vie quotidienne. Leur excellente capacité à dissiper de l'énergie en fait également des matériaux très utilisés dans le domaine militaire pour atténuer les ondes de souffle émises lors d'une explosion. De nombreuses études sur les cinquante dernières années ont identifié plusieurs mécanismes d'atténuation, cependant sans contrôle précis des paramètres de la mousse. L'effet de chaque paramètre de la mousse et de l'onde sur l'atténuation reste donc une question ouverte. Dans cet article, nous étudions l'effet de la fraction liquide d'une mousse sur l'atténuation d'une onde de choc créée par un tube à choc. Nous mettons en œuvre une nouvelle méthode expérimentale permettant de cartographier la fraction liquide en dynamique. Les variations de ce paramètre dans le temps sont reliées au comportement du signal de pression dans la mousse. L'étude est complétée par une approche numérique, modélisant la propagation d'une onde de choc dans un milieu effectif non-newtonien.

Abstract

Liquid foams, dispersion of a gaseous phase inside a liquid phase, are used for many applications. Due to their excellent ability to dissipate energy, these materials are namely used to mitigate blast effects. Over the past fifty years, several attenuation mechanisms were identified, however the foam parameters are poorly controlled in most of the studies. The effect of each parameter of the foam or the wave on the attenuation is therefore still an open question. In this paper, we study the effect of the liquid fraction of a foam with constant bubble size on the attenuation of a shock wave created with a shock tube. We use a new experimental method to map the dynamical liquid fraction. The variations of that parameter in time are linked to the pressure wave behaviour inside the foam. The study is completed with a numerical approach, modelling the propagation of a shock wave in an effective, non-newtonian fluid.

Keywords: liquid foam; shock wave; attenuation; effective medium

1 Introduction

Liquid foams consist of a dense packing a gas bubbles, separated by a continuous liquid phase containing surfactants. Such materials are used in a wide range of applications, e.g. food industry or cosmetics [1], oil recovery [2], or in the military domain for blast wave mitigation [3]. This latter subject has received a considerable attention for several decades, and many studies showed the great ability of foams to attenuate the effects of explosions, namely blast waves [4, 5, 6] and fragment propagation [7].

Several attenuation mechanisms were identified over the years, such as heat transfer between phases [8, 9], fragmentation of the liquid films into droplets [3, 10], and shock wave dispersion, thickening, and refraction. More recent studies showed the influence of the bubble size and thermal dissipation on the attenuation of moderate blast waves in liquid foams with controlled liquid fraction and chemical composition [16, 17]. In most of the available literature, the foam parameters are either poorly controlled because of the important volumes of foams which were used, or not clearly specified by the authors. The characterisation of all those effects as a function of the shock wave and the foam properties is therefore still unclear and remains an important challenge.

Modelling the shock wave propagation in a highly deformable, visco-elasto-plastic, two-phase medium, is a complicated task. The Effective Gas Flow (EGF) model assumes an ideal gas-like behaviour for the foam [11, 12]. This model solves Euler's equations and neglects dispersion and dissipation rates [3]. On the contrary, the Gas Droplet Flow (GDF) and the Dusty Gas Droplet (DGD) numerical models are based on the assumption that the foam is instantaneously atomised into a spray of water droplets [10, 13, 14]. The equations of motion are solved for the gas and the liquid phases, adding a relative drag force between the droplets and the air in motion. Up to now, the macroscopic rheological properties of foams have never been taken into account in any model. And yet, the effective viscosity of a foam can be several orders of magnitude higher than that of the foaming solution [15], therefore showing the need to enquire about the possible link between the shock wave attenuation and the effective properties of a foam.

In this paper, we investigate the role of the foam liquid fraction on the attenuation of a shock wave created with a shock tube. We use a foam generation and characterisation system to allow an independent control of the foam parameters. All the foams used in our study therefore have the same bubble size and chemical composition. We first present new experimental methods and results on the dynamical measurement of the foam liquid fraction. We relate our experimental results to the pressure wave behaviour inside the foam. We then study the link between the shock attenuation in the foam and the rheological and thermodynamical properties of the foam. To do so, we develop a numerical approach, modelling the propagation of a shock wave in an effective, non-newtonian fluid, disregarding the foam structure and the potential foam rupture at early stages.

2 Experimental methods

2.1 Foam characterisation

The foaming solution is made of sodium dodecylsulfate (SDS) at a concentration of 7 $g{\cdot}L^{-1}$, and glycerol (10 % vol.). The foam is then produced using the setup shown in Figure 1. The liquid fraction Φ, defined as the ratio of the volume of liquid to the total volume of foam, is controlled by a balance between the

gas and the solution flow rates. It is measured for each experiment by weighing a known volume of foam. In this study, we explore three distinct values of Φ: 2 %, 5 %, and 8 %.

The bubble size of the foam is characterised by sampling a few hundred of bubbles from a small volume of foam. They are then spread on a thin layer of foaming solution, forming a monolayer of spherical bubbles. Their average radius R is determined by image processing and is used to quantify the bubble size in the foam. In the whole study, the bubble size is kept constant and is $R_0 = (180 \pm 10)$ µm. The dynamical liquid fraction Φ'

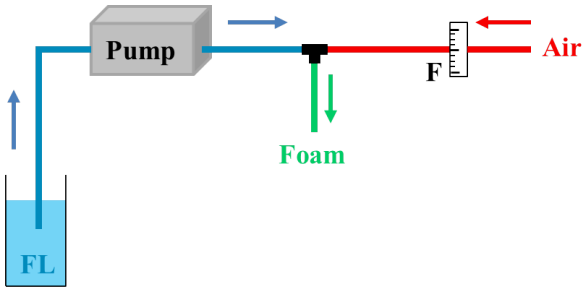

Figure 1: Sketch of the foam generation setup. The foaming liquid (FL) is pumped with a pump which can be tuned in amplitude and frequency. It mixes with air at a T-junction, creating some foam. The air flux is controlled with a flowmeter (F), allowing to vary the foam liquid fraction.

2.2 Shock tube

Shock waves are generated with a shock tube, whose square section is 80 mm × 80 mm. It is composed of a high-pressure chamber separated from a low-pressure chamber by a diaphragm. Air is injected in the high-pressure chamber until the rupture of the diaphragm, which creates a shock wave that propagates in the tube. The diaphragm was a 75 µm thick mylar sheet. The pressure at which the diaphragm bursts dictates the shock characteristics, namely its Mach number $\mathcal{M} = \frac{V}{a}$, where V is the shock wave velocity, and a is the speed of sound of the medium at rest. In all our experiments, this parameter is kept constant and is, in air, $\mathcal{M} = (1.43 \pm 0.03)$.

The end of the tube has a thinner (10 mm wide, 80 mm heigh) and transparent part, filled with foam, to allow visualisation of the shock-foam interaction with a high-speed camera, as shown in Figure 2. That part of the tube is equipped of a removable blade, ensuring an air/foam interface as flat as possible. Seven pressure sensors PCB 113 B28 or 113 B21 are installed on the tube and record the overpressure $p(t)$ in the foam. For given foam parameters (liquid fraction and bubble size), the shock amplitude in the foam varie by less than 10 % from one experiment to another. The characteristic duration of an experiment, between the foam injection in the tube and the shock wave generation, is of the order of 1 to 3 minutes. Typical pressure signals, recorded in air and in the foam are shown in Figure 3.

2.3 Foam evolution in time

Due to drainage and coarsening, both the foam liquid fraction and average bubble size depend on time [18]. The foam drainage velocity is [19]

$$u_{\text{drainage}} = \frac{4\mathcal{K}}{7.3} \frac{\rho_\ell \, g \, R^2}{\mu} \sqrt{\Phi}, \tag{1}$$

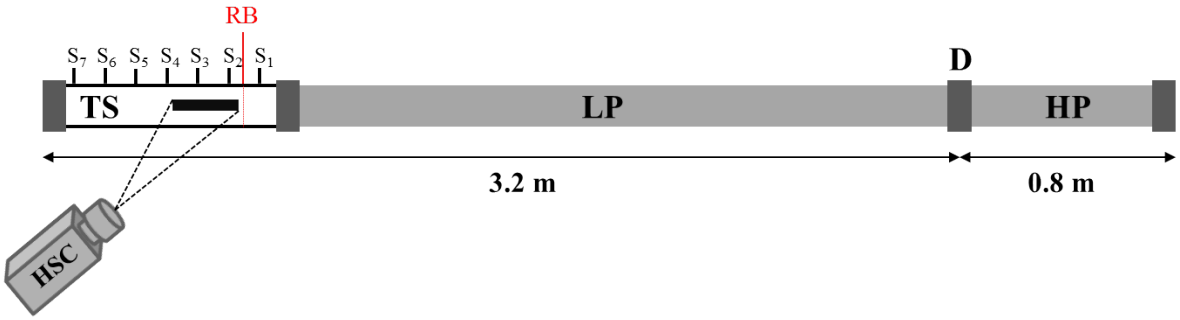

Figure 2: Side view of the shock tube apparatus. The high-pressure (HP) and low-pressure (LP) chambers are separated by a mylar diaphragm (D). The end of the tube has a transparent section (TS), filled with foam up to the removable blade (RB), where a high-speed camera (HSC) Photron SA-X2 records the shock/foam interaction. Pressure sensors are measuring the pressure field in air (S_1) and inside the foam (S_2 to S_7). The distance between two consecutive sensors is 10 cm. The black rectangle in the TS area represents the visualisation field.

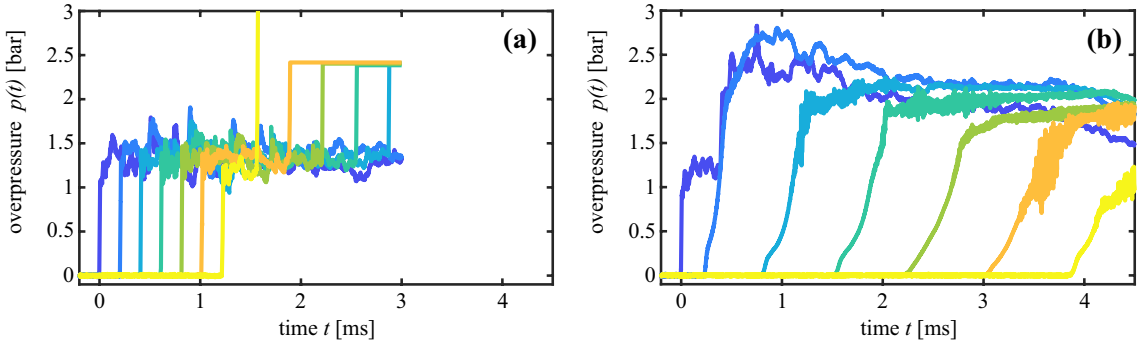

Figure 3: **(a)** Typical pressure measurements in air. **(b)** Typical pressure measurements in a liquid foam whose liquid fraction was $\Phi = 8\,\%$. The time and pressure scales were left identical on purpose.

where $\mathcal{K} \simeq 0.0035$; $g = 9.81\,\mathrm{m/s^2}$; $\rho_\ell = 1000\,\mathrm{kg/m^3}$ and $\mu \simeq 10^{-3}\,\mathrm{Pa{\cdot}s}$ are respectively the density and the viscosity of the foaming solution. In our typical experimental conditions, $\Phi \sim 0.05$ and $R \sim 150\,\mu\mathrm{m}$, leading to a typical drainage velocity $u_{\mathrm{drainage}} \sim 0.1\,\mathrm{mm/s}$. The characteristic time for which a significant change in liquid fraction is observed is then $\tau_{\mathrm{drainage}} \sim \frac{H}{u_{\mathrm{drainage}}} \sim 13\,\mathrm{min}$, where $H = 80\,\mathrm{mm}$ is the height of the foam sample inside the shock tube. The pressure measurements, made at the top of the cell, are therefore representative of the global pressure wave propagating through the whole cross-sectional area.

The coarsening dynamics has been characterised for each liquid fraction explored in this study. A typical result is shown in Figure 4. By choosing a waiting time, we can therefore set the bubble size, and vary the liquid fraction of the foam independently of that parameter.

3 Dynamical evolution of the foam liquid fraction

Figure 5 shows the foam response to a shock wave. When the shock enters the foam, the gas bubbles are either deformed of destroyed due to the liquid film bursting. This leads to a dynamical change in the foam structure, whose signature is the propagation of a darker area in Figure 5. The typical time scale for a liquid film to burst is of the order of 1 ms [20]. At short times, that is to say $t \lesssim 0.1$ ms, the bubbles are therefore deformed but intact.

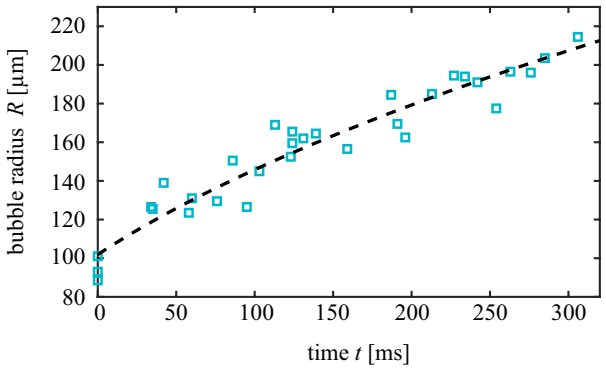

Figure 4: Typical bubble size evolution in time for a foam whose liquid fraction was $\Phi = 5\,\%$. The squares are experimental data points. The data are fitted with a coarsening law (dashed line) $R(t) = R^*\sqrt{1+\frac{t}{t_c}}$, with $R^* = 102\,\mu$m and $t_c = 95\,$s.

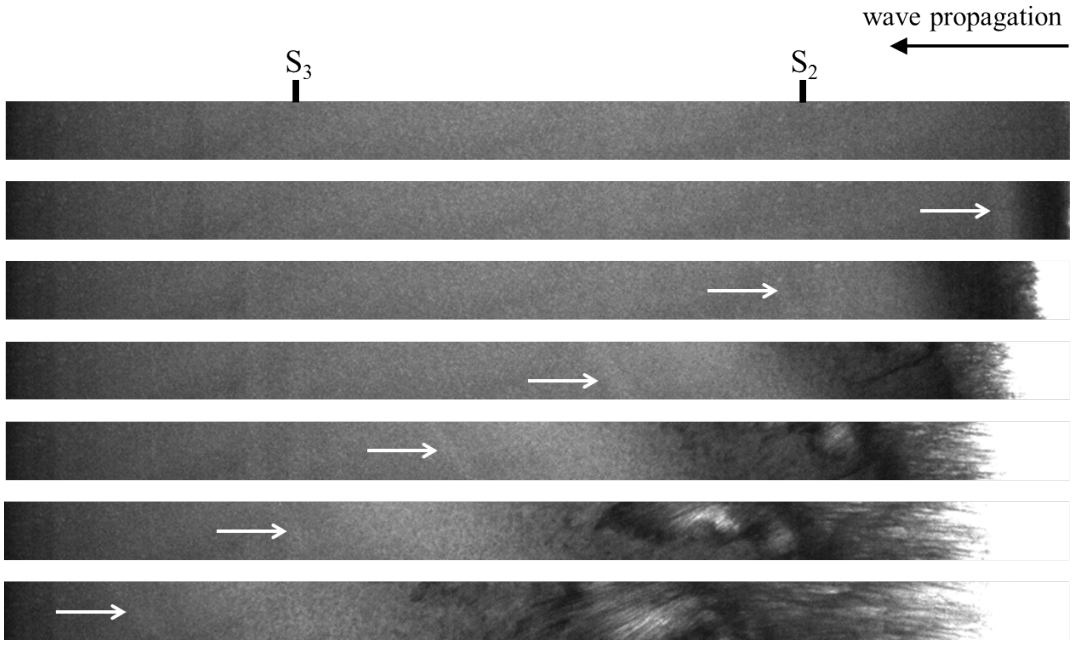

Figure 5: Chronophotography of the shock/foam interaction for a liquid fraction $\Phi = 5\,\%$. The time step between each frame is 17 µs. The first image shows the foam at rest and the locations of pressure sensors S_2 and S_3, the distance between which being 10 cm. The tip of each white arrow shows the shock front propagating in the foam. The dark area propagating from right to left is due to a dynamical change of the foam properties. The corresponding liquid fraction is given by eq.(3).

Light transmission in foams is governed by the multiple scattering of light at the air/liquid interfaces. In the case where the thickness of the foam sample $W = 1.5\,$cm is much larger than the transport mean free path $\ell^* = 2\frac{R}{\sqrt{\Phi}} \simeq 1.5\,$mm, the transmission factor can be expressed as [21]

$$\tau = \frac{R}{W}\left(\frac{\alpha+\beta\,\Phi}{\sqrt{\Phi}}\right), \tag{2}$$

where $\alpha = 3.48$ and $\beta = 6.88$.

For bubble radii lying in the range $[50;350]$ µm, the thermal boundary layer thickness is much larger

than the bubble size, and the compression of the bubble can be considered as nearly isothermal [16, 22, 23]. Assuming an ideal gas behaviour inside the bubbles, the volume of a compressed bubble reads $\mathcal{V}' = \frac{P_0}{P'}\,\mathcal{V}_0$, where P_0 is the absolute ambient pressure in the foam before the shock, P' is the maximal absolute pressure inside the foam after the shock, and $\mathcal{V}_0$ is the volume of a bubble at rest. Given that $P' \simeq 3P_0$ for all the experiments, the compressed bubble radius is therefore $R' \simeq 0.7\,R_0 \simeq 125\,\mu\text{m}$. We can calculate the transmission coefficient for each frame, and, under that assumption, the dynamical liquid fraction Φ' therefore satisfies

$$\Phi'^2 + \left(2\frac{\alpha}{\beta} - \frac{\tau'^2\,W^2}{R'^2\,\beta^2}\right)\Phi' + \frac{\alpha^2}{\beta^2} = 0, \tag{3}$$

where τ' and R' are the transmission coefficient and the bubble size of the foam in the shocked state.

Figure 6 shows a typical liquid fraction mapping. We observe a significant increase in liquid fraction after the shock had passed. For all the experiments, the dynamical liquid fraction increases up to nearly 20 %. The foam in that region therefore almost behaves as a bubbly liquid, whose mechanical and rheological properties are very different from dry foams [18].

Whatever the initial liquid fraction of the foam, the pressure wave recorded in the foam exhibits a slope rupture (Figure 7): the pressure rises quickly over a short amount of time, typically 0.03 ms, and suddenly increases less rapidly. Figure 7 shows that the arrival time of the dense liquid area somewhat matches with the time at which the pressure gradient changes. That slope rupture, described in previous studies as a shock precursor [3], could therefore be explained by a significant dynamical change of the foam properties: at early stages, the wave propagates in a foam whose characteristics are the initial ones; at later stages, it propagates in a high liquid fraction medium, where $\Phi' \simeq 20\,\%$.

It was recently shown that the propagation of linear acoustic waves in foams was dispersive, the dispersion relation depending on bubble size and liquid fraction [24]. Understanding the link between dispersion of highly non-linear waves in foams and the dynamical change in liquid fraction is still under investigation, and would help unravel the shock wave dynamics and attenuation in foams.

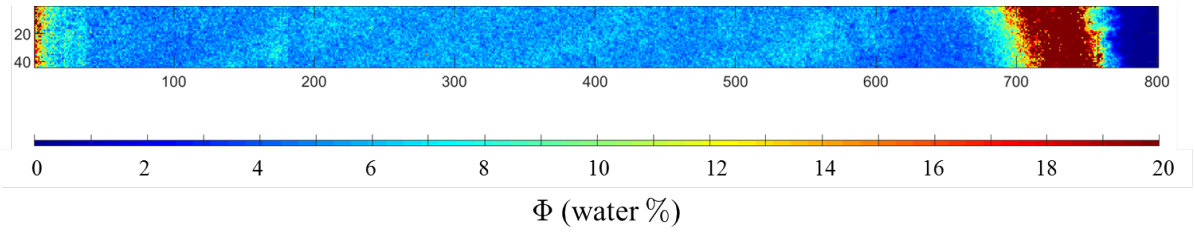

Figure 6: Example of liquid fraction mapping at $t = 0.35$ ms for a foam whose initial liquid fraction was $\Phi = 5\,\%$. A local, dynamical change in liquid fraction is visible on the right, and propagates behind the shock. The width of the region of interest is 20 cm, its height is 1 cm. The colour variations on the extreme left of the picture is an artifact.

4 Numerical simulations

In this section, we present our numerical model to simulate a shock propagation in a foam. Contrary to previous studies, we consider that the foam remains intact at early stages. We describe the foam as an effective, non-newtonian fluid, whose properties are computed in subsections 4.1 and 4.2.

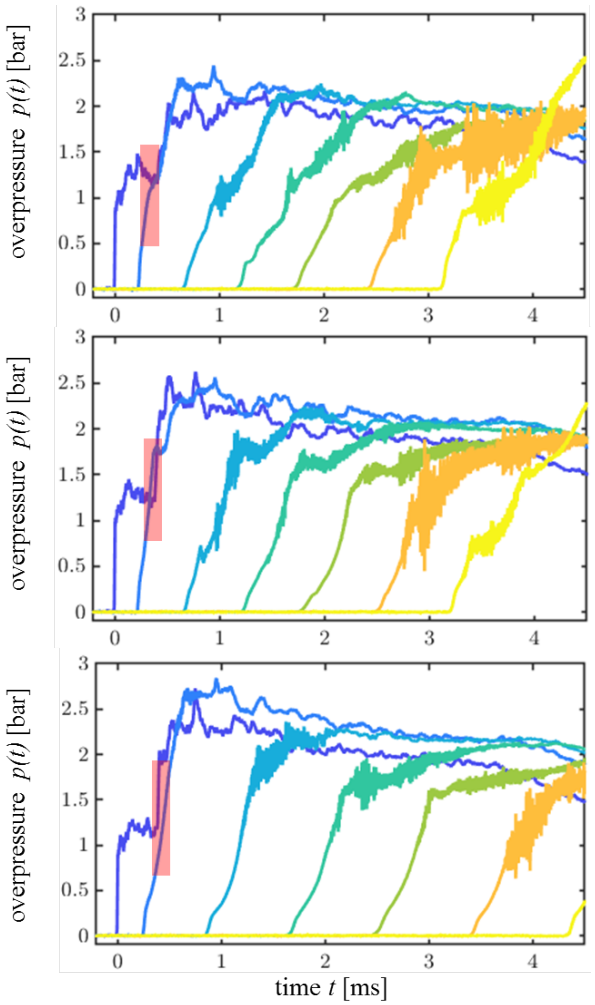

Figure 7: Experimental pressure signals for liquid fractions of 2 % (top), 5 % (middle), and 8 % (bottom). The red rectangle illustrates the time window where the dense liquid front passes at sensor S_2. The width of the rectangle corresponds to the errorbar on the arrival time.

4.1 Mixture law

The characteristic spreading length of the shock front is $\lambda = V_{\text{sf}} \times t_{\text{rise}}$, where $V_{\text{sf}} \simeq 100\,\text{m/s}$ is the shock velocity in the foam, and $t_{\text{rise}} \simeq 1\,\text{ms}$ is the pressure rise time in the foam. Therefore, $\lambda \simeq 0.1\,\text{m}$, that is to say $\lambda \gg R$. In that limit, the foam can be considered as an effective medium, disregarding its structure.

We therefore model the foam using the mixture law [25], defining an effective density $\rho_{\text{f}} = \Phi\,\rho_\ell + (1-\Phi)\,\rho_{\text{g}}$, and an effective compressibility $\chi_{\text{f}} = \Phi\,\chi_\ell + (1-\Phi)\chi_{\text{g}}$, where ρ_{g} is the density of the gaseous phase, χ_ℓ the compressibility of the liquid phase, and χ_{g} that of the gas phase. The sound velocity in the foam is thus given by

$$c_{\text{f}} = \sqrt{\frac{1}{\rho_{\text{f}}\,\chi_{\text{f}}}}, \tag{4}$$

and lies in the range $[40-70]$ m/s for the explored liquid fraction interval.

4.2 Effective viscosity

Foams are non-newtonian, shear-thinning fluids. Their effective viscosity depends on the shear rate, and is well decribed by Herschel-Bulkley's law [15]:

$$\mu_{\mathrm{f}}(\dot{\gamma}) = k\,\dot{\gamma}^{n-1}, \tag{5}$$

where $\dot{\gamma}$ is the shear rate, k is the consistency factor, and $n < 1$. For SDS foams, the power-law exponent is $n = 0.42$, and the consistency factor depends on the liquid fraction and the bubble size [26]. Table 1 gives the values of k for the three liquid fractions investigated in this study.

Φ [liquid %]	k
2	15
5	8
8	4

Table 1: Values of the consistency factor k for various liquid fractions.

4.3 Numerical model

Given the high gas fractions in our foams, we used an ideal gas equation of state for the numerical model, reading $P = \rho_{\mathrm{f}}\, r\, T$, where $r = \frac{R}{\mathcal{M}_{\mathrm{f}}}$ is the reduced ideal gas constant; $\mathcal{M}_{\mathrm{f}}$ being the molecular mass of the foam, of the order of 1 kg/mol.

We used the finite volume code Star CCM$^+$ to simulate a shock propagation in a foam inside a shock tube having the same characteristics as the one used in our experiments. The foam is modelled as an effective medium satisfying the ideal gas equation of state, and characterised by its effective density ρ_{f}, compressibility χ_{f}, and viscosity $\mu_{\mathrm{f}}(\dot{\gamma})$. The simulation were run with a coupled flow solver, and an implicit, unsteady scheme. The time step between each iteration is set to 10 µs.

We only simulate the shock propagation in the foam volume. The initial condition is therefore taken to be the mean experimental pressure signal in air at sensor S_1 just before the wave enters the foam.

Figure 8 shows the comparison between experimental and numerical pressure signals. For $\Phi = 2\,\%$ and $5\,\%$, the numerical pressure behaviour at sensor S_2 is in good agreement with the experimental signal. For $\Phi = 8\,\%$, the simulation does not capture the change in slope observed in the experiments.

Deeper in the foam sample (sensors S_3 to S_7), we note a significant discrepancy between the experimental signals and the simulations. In the experiments, the pressure wave decelerates in the foam to eventually reach a constant velocity corresponding to the sound velocity in the foam. This effect is never observed in the simulations, whatever the liquid fraction. On the contrary, the wave immediately propagates at the sound velocity of the effective medium. Moreover, experiments show a significant signal spreading inside the foam. For dry foams ($\Phi = 2\,\%$), simulations also exhibit a signal spreading but not as important as the experimental one. For wetter foams, the numerical pressure rise remains steep and no significant spreading is observed.

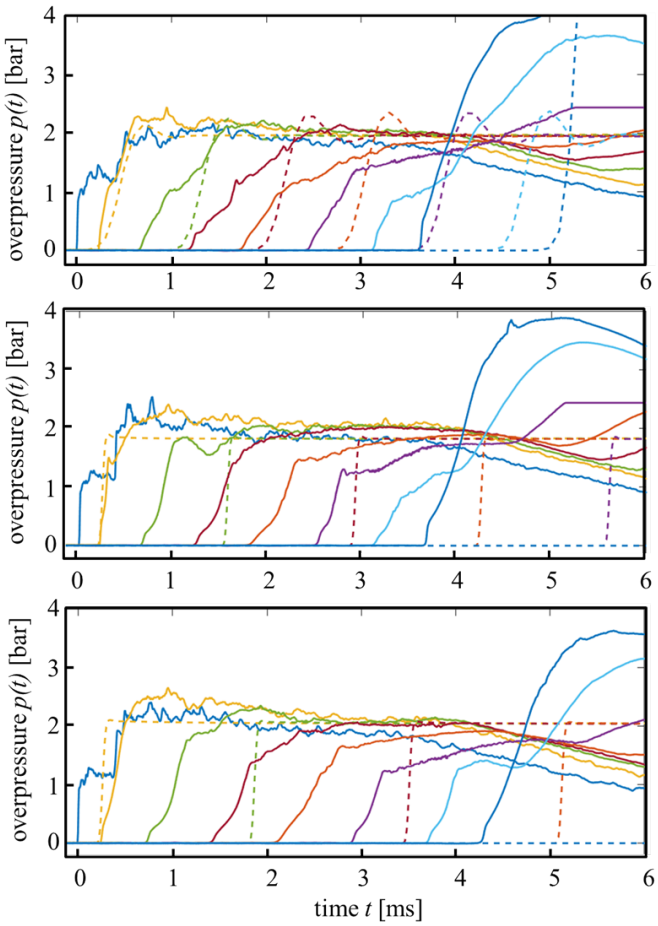

Figure 8: Comparison between experimental (solid lines) and numerical (dashed lines) pressure signals for a shock propagation in a foam whose liquid fraction is $\Phi = 2\,\%$ (top), $5\,\%$ (middle), and $8\,\%$ (bottom).

5 Conclusion

We reported new results on the interaction of a shock wave and a liquid foam. By controlling the foam parameters independently from one another, we investigated the role of the foam liquid fraction on the pressure wave behaviour inside the foam. We developped a new experimental method to measure the dynamical liquid fraction, and showed that the foam was undergoing a significant increase in liquid fraction after the shock had passed. This liquid content variation was correlated to the slope rupture observed on the pressure signals. Those results bring new information to understand how foams attenuate blast waves.

The study was completed by a numerical approach. We simulated the propagation of a shock wave in a foam, describing the latter as an effective non-newtonian fluid. Despite a good agreement with the experiments at the beginning of the propagation, the main features of the signal could not be recovered in the simulations, such as the wave deceleration and the signal spreading. This aspect is currently being investigated deeper into details.

In that purpose, we are namely running new experiments with a foam whose rheological properties are significantly different from that used in the present study. Those new results will widen the range of explored parameters, and will allow to check wether the numerical model and main assumptions need to be refined.

References

[1] P. Stevenson, editor. *Foam Engineering: Fundamentals and Applications*, Wiley, 2012.

[2] P. Grassia *et al.*, Analysis of a model for foam oil improved recovery, *J. Fluid Mech.*, **751** (2014) 346–405.

[3] A. Britan *et al.*, Macro-mechanical modelling of blast wave mitigation in foams. Part I: review of available experiments and models, *Shock Waves*, **23** (2013) 5–23.

[4] F. H. Winfield, D. A. Hill, Preliminary research on the properties of aqueous foams and their blast attenuation characteristics, Technical Report, Defense Research Establishment, Alberta, Canada (1977).

[5] R. Raspet, S. K. Griffiths, The reduction of blast noise with aqueous foams, *J. Acoust. Soc. Am.*, **74** (1983) 1757–1763.

[6] W. F. Hartman, B. A. Boughton, M. E. Larsen, Blast Mitigation Capabilities of Aqueous Foams, Technical Report, Sandia National Laboratories (2006).

[7] J. S. Krasinski, Some aspects of the fluid dynamics of liquid-air foams of high dryness fraction, *Prog. Aerospace Sci.* **29** (1993) 125–163.

[8] I. Goldfarb, I. R. Schreiber, F. I. Vafina, Heat transfer effect on sound propagation in foam, *J. Acoust. Soc. Am.*, **92** (1992) 2756–2769.

[9] I. Goldfarb *et al.*, Sound and weak shock wave propagation in gas-liquid foams, *Shock Waves*, **7** (1997) 77–88.

[10] E. Del Prete *et al.*, Blast wave mitigation by dry aqueous foams, *Shock Waves*, **23** (2013) 39–53.

[11] G. Rudinger, Some Properties of Shock Relaxation in Gas Flows Carrying Small Particles, *Phys. Fluids*, **7** (1964) 658.

[12] V. M. Kudinov *et al.*, Shock waves in gas-liquid foams, *Appl. Mech.*, **13** (1977) 279–283.

[13] A. B. Britan, E. I. Vasilev, B. A. Kulikosvky, Modeling the process of shock wave attenuation by a foam screen, *Shock Waves*, **30** (1994) 389–396.

[14] O. Igra, G. Ben-Dor, Dusty Shock Waves, *Appl. Mech. Rev.*, **41** (1988).

[15] A. D. Gopal, D. J. Durian, Shear-Induced "Melting" of an Aqueous Foam, *J. Colloid Interface Sci.*, **213** (1999) 169–178.

[16] M. Monloubou *et al.*, Influence of bubble size and thermal dissipation on compressive wave attenuation in liquid foams, *EPJE*, **112** (2015) 34001.

[17] M. Monloubou *et al.*, Blast wave attenuation in liquid foams: role of gas and evidence of an optimal bubble size, *Soft Matter*, **12** (2016) 8015–8024.

[18] I. Cantat *et al.*, *Foams, Structure and Dynamics*, Oxford University Press, 2013.

[19] A. Saint-Jalmes, Y. Zhang, D. Langevin, Quantitative description of foam drainage: Transitions with surface mobility, *EPJE*, **15** (2004) 53–60.

[20] N. BrÃĺmond, E. Villermaux, Bursting thin liquid films, *J. Fluid Mech.*, **524** (2005) 121–130.

[21] M. U. Vera, A. Saint-Jalmes, D. J. Durian, Scattering optics of foams, *Appl. Opt.*, **40** (2001) 4210.

[22] A. Propsperetti, The thermal behaviour of oscillating gas bubbles, *J. Fluid Mech.*, **222** (1991) 587–616.

[23] N. Mujica, S. Fauve, Sound velocity and absoprtion in a coarsening foam, *Phys. Rev. E*, **66** (2002) 021404.

[24] J. Pierre, B. Dollet, V. Leroy, Resonant Acoustic Propagation and Negative Density in Liquid Foams, *Phys. Rev. Lett.*, **112** (2014) 148307.

[25] A. B. Wood, *A Textbook of Sound*, MacMillan, New-York, 1930

[26] S. Marze, D. Langevin, A. Saint-Jalmes, Aqueous foams slip and shear regimes determined by rheometry and multiple light scattering, *J. Rheol.*, **52** (2008) 1091–1111.